

R Measurements at High Q^2

F.A. Harris
University of Hawaii, Honolulu

Previous measurements of $R = \sigma(e^+e^- \rightarrow \text{hadrons})/\sigma(e^+e^- \rightarrow \mu^+\mu^-)$ at high Q^2 are reviewed. Recent R measurement results, including those from the Beijing Spectrometer Experiment, are described. The present status of R measurements and future measurement possibilities are summarized.

1. INTRODUCTION

The QED running coupling constant evaluated at the Z pole, $\alpha(M_Z^2)$, and the anomalous magnetic moment of the muon, $a_\mu = (g - 2)/2$, are two fundamental quantities that are used to test the Standard Model (SM). The dominant uncertainties in both $\alpha(M_Z^2)$ and a_μ^{SM} are due to the effects of hadronic vacuum polarization, which cannot be reliably calculated in the low energy region. Instead, with the application of dispersion relations, experimentally measured R values are used to determine the vacuum polarization, where R is the lowest order cross section for $e^+e^- \rightarrow \gamma^* \rightarrow \text{hadrons}$ in units of the lowest-order QED cross section for $e^+e^- \rightarrow \mu^+\mu^-$, namely $R = \sigma(e^+e^- \rightarrow \text{hadrons})/\sigma(e^+e^- \rightarrow \mu^+\mu^-)$, where $\sigma(e^+e^- \rightarrow \mu^+\mu^-) = \sigma_{\mu\mu}^0 = 4\pi\alpha^2(0)/3s$. Improved precision for $\alpha(M_Z^2)$ also narrows the allowed range of the Higgs mass prediction using electro weak loop corrections. For much more detail on the importance of R measurements [1–3].

The uncertainty in $\alpha(M_Z^2)$ is introduced when it is extrapolated to the Z -pole.

$$\alpha(q^2) = \frac{\alpha_0}{1 - \Delta\alpha(q^2)},$$

where α_0 is the fine structure constant, which is known very precisely, and $\Delta\alpha(q^2)$ is the vacuum polarization term.

$$\Delta\alpha(q^2) = \Delta\alpha_l(q^2) + \Delta_{\text{had}}^{(5)}\alpha(q^2) + \Delta_{\text{top}}\alpha(q^2).$$

The leptonic vacuum polarization, $\Delta\alpha_l(q^2)$, can be calculated theoretically, and the top contribution, $\Delta_{\text{top}}\alpha(q^2)$ is absorbed as a parameter in the SM fit. The dominant uncertainty is then due to the effects of hadronic vacuum polarization, $\Delta_{\text{had}}^{(5)}$, which is calculated with experimentally determined R values using dispersion relations.

Here, R measurements above the center-of-mass (cm) energy corresponding to the J/ψ are reviewed. R measurements at lower energy are described in [3, 4]. Since the theoretical $a_\mu = (g - 2)/2$ is more dependent on low energy than on high energy R values, we will concern ourselves here primarily with

the effect of R measurements on $\alpha(q^2)$. In the following sections, previous R measurements will be summarized, recent measurements by the Beijing Spectrometer Experiment (BES) and CLEO will be described, and the current R status will be reviewed.

2. PREVIOUS R MEASUREMENTS

Figure 1 shows the summary of R measurements as summarized by the Particle Data Group [5]. These are selected measurements; older measurements with even larger errors are not shown. Also, systematic normalization errors (5–20%) are not included on the points shown.

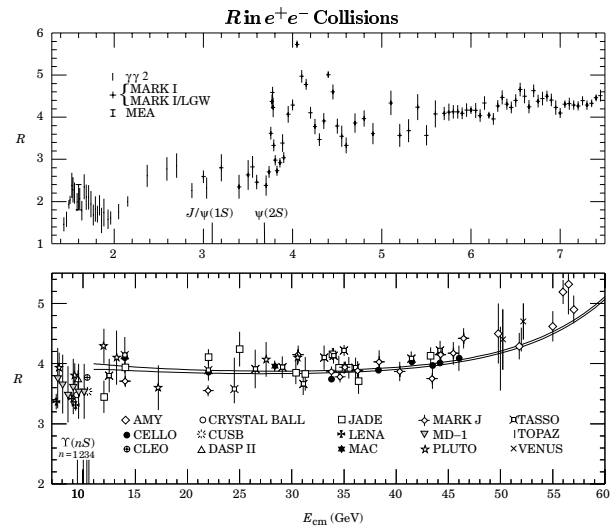


Figure 1: Summary of R values from PDG2000 [5]. Some older measurements with even larger errors are not shown. Systematic normalization errors (5–20 %) are not included on the points shown.

We will be primarily interested in the center of mass (cm) energy region $m_{J/\psi} < E_{\text{cm}} < 12$ GeV. For higher energies,

perturbative QCD (PQCD) can be used to describe the behavior of R as a function of energy [6]. Analyses that use data below ~ 12 GeV are “data driven” approaches [6]; “theory driven” approaches use PQCD to go much lower in energy [8]. Although less dependent on the quality of experimental data, the latter must make additional theoretical assumptions.

Figure 2 shows a 1995 summary plot of the cm energy region below 10 GeV [9]. The R values used as a function of energy to evaluate the dispersion integral are indicated by the smooth line through the points, and the R value uncertainties ascribed in the various energy regions are indicated by the bands. In the 1 to 5 GeV region, the R uncertainty is taken to be 15%. Note that the Crystal Ball data [7] used in the 5 to 7 GeV region is unpublished.

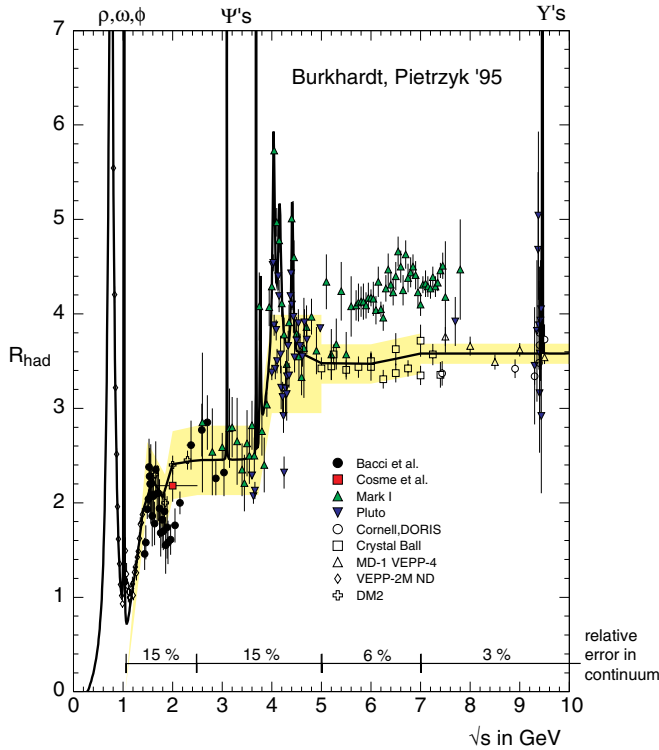


Figure 2: Summary of 1995 R values from [9]. The uncertainties in the various energy regions are shown by the bands and given at the bottom of the figure.

3. BES R MEASUREMENT

Recently a detailed R scan was completed by the upgraded Beijing Spectrometer (BES-II) Experiment [10]. The analysis is described in some detail here to demonstrate the complexity of R measurements. BESII is a general purpose solenoidal detector located at the Beijing Electron Positron Collider (BEPC), which is the only facility operating in the CM energy range from 2 to 5 GeV. The luminosity at the J/ψ is $\sim 5 \times 10^{30}$ $\text{cm}^{-2}\text{s}^{-1}$. BESII is described in detail elsewhere [11].

Experimentally, the value of R is determined from the number of observed hadronic events, $N_{\text{had}}^{\text{obs}}$, by the relation

$$R = \frac{N_{\text{had}}^{\text{obs}} - N_{bg} - \sum_l N_{ll} - N_{\gamma\gamma}}{\sigma_{\mu\mu}^0 \cdot L \cdot \varepsilon_{\text{had}} \cdot \varepsilon_{\text{trg}} \cdot (1 + \delta)}, \quad (1)$$

where N_{bg} is the number of beam-associated background events; $\sum_l N_{ll}$, ($l = e, \mu, \tau$) are the numbers of lepton-pair events from one-photon processes and $N_{\gamma\gamma}$ the number of two-photon process events that are misidentified as hadronic events; L is the integrated luminosity; δ is the radiative correction; ε_{had} is the detection efficiency for hadronic events; and ε_{trg} is the trigger efficiency.

In 1998 BES performed an initial measurement of R using six scan points: 2.6, 3.2, 3.4, 3.55, 4.6, and 5.0 GeV [12]. At each point separated beam runs were done for the study of beam gas background. In 1999, BES measured 85 scan points with ~ 1000 hadronic events per point. Separated beam running was done at 24 energy points, while single beam running was done at 7 points [10].

3.1. Event Selection

The main sources of background for this measurement are cosmic rays, lepton pair production, two-photon processes and single-beam associated processes. Clear Bhabha events are first rejected. Then the hadronic events are selected based on charged track information. Special attention is paid to two-prong events, where cosmic ray and lepton pair backgrounds are especially severe, and additional requirements are imposed to provide extra background rejection [12].

An acceptable charged track must be in the polar angle region $|\cos \theta| < 0.84$, have a good helix fit, and not be clearly identified as an electron or muon. The distance of closest approach to the beam axis must be less than 2 cm in the transverse plane, and must occur at a point along the beam axis for which $|z| < 18$ cm. In addition, the following criteria must be satisfied: (i) $p < p_{\text{beam}} + 5 \times \sigma_p$, where p and p_{beam} are the track and incident beam momenta, respectively, and σ_p is the momentum uncertainty for a charged track for which $p = p_{\text{beam}}$; (ii) $E < 0.6E_{\text{beam}}$, where E is the barrel shower counter (BSC) energy associated with the track, and E_{beam} is the beam energy; (iii) $2 < t < t_p + 5 \times \sigma_t$ (in ns.), where t is the measured time-of-flight for the track, t_p is the time-of-flight calculated assigning the proton mass to the track, and σ_t is the resolution of the barrel time-of-flight system.

After track selection, event selection requires the presence of at least two charged tracks, of which at least one satisfies all of the criteria listed above. In addition, the total energy deposited in the BSC (E_{sum}) must be greater than $0.28E_{\text{beam}}$, and the selected tracks must not all point into the forward ($\cos \theta > 0$) or the backward ($\cos \theta < 0$) hemisphere.

For two-prong events, residual cosmic ray and lepton pair (e^+e^- and $\mu^+\mu^-$) backgrounds are removed by requiring that the tracks not be back-to-back, and that there be at least two isolated energy clusters in the BSC with $E > 100$ MeV that are at least 15° in azimuth from the closest charged track. This last requirement rejects radiative Bhabha events.

These requirements eliminate virtually all cosmic rays and most of the lepton pair (e^+e^- and $\mu^+\mu^-$) events. The remaining background contributions due to lepton pairs (N_{ll}), including $\tau^+\tau^-$ production above threshold, and two-photon events ($N_{\gamma\gamma}$) are estimated using Monte Carlo simulations and subtracted as indicated in Eq. (1).

Cuts used for selecting hadronic events were varied in a wide range, e.g. $\cos\theta$ from 0.75 to 0.90, E_{sum} from $0.24E_{\text{beam}}$ to $0.32E_{\text{beam}}$, to estimate the systematic error arising from the event selection, which turned out to be the dominant systematic error as indicated in Table II.

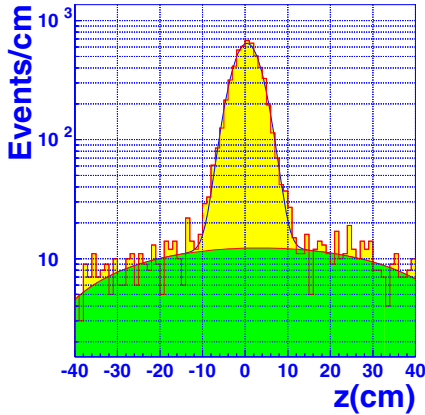


Figure 3: Distribution of event vertices along the beam line (z). A gaussian is used to describe the real beam events, while a polynomial of degree two is used to describe beam associated background.

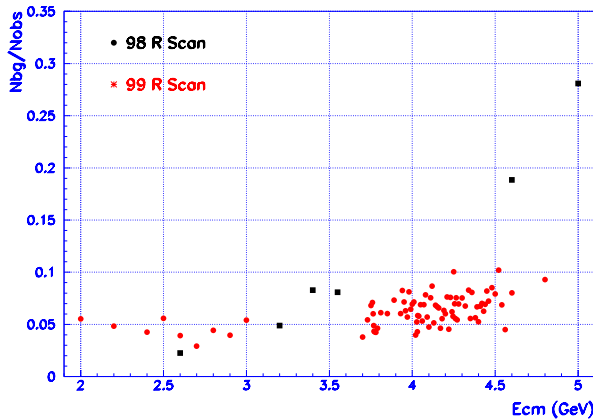


Figure 4: Amount of beam associated background versus scan energy.

3.2. Beam Associated Background

The largest background is due to beam associated background, N_{bg} . To determine the level of single-beam-induced backgrounds, the same hadronic event selection criteria are applied to separated-beam data, and the number of separated-beam events, N_{sep} , surviving these criteria is obtained. The

number of beam-associated background events, N_{bg} , in the corresponding hadronic event sample is given by $N_{\text{bg}} = f \times N_{\text{sep}}$, where f is the ratio of the products of the pressure at the collision region and the integrated beam current for colliding and separated-beam runs.

The beam-associated background can also be determined by fitting the distribution of event vertices along the beam direction with a Gaussian for real hadronic events and a polynomial of degree two for the background, as shown in Figure 3. This was the primary method used for the 1999 data. Figure 4 shows the amount of beam associated background versus the scan energy. The differences between R values obtained using these two methods to determine the beam-associated background range between 0.3 and 2.3%, depending on the energy. These differences are included in the systematic uncertainty.

3.3. Hadron Efficiency

JETSET, the Monte Carlo event generator that is commonly used to simulate $e^+e^- \rightarrow \text{hadrons}$, was not intended to be applicable to the low energy region, especially that below 3 GeV. A special joint effort was made by the Lund group and the BES collaboration to develop the LUARLW generator, which uses a formalism based on the Lund Model Area Law, but without the extreme-high-energy approximations used in JETSET's string fragmentation algorithm [13, 14]. The final states simulated in LUARLW are exclusive in contrast to JETSET, where they are inclusive. In addition, LUARLW uses fewer free parameters in the fragmentation function than JETSET. Above 3.77 GeV, the production of D , D^* , D_s , and D_s^* is included in the generator according to the Eichten Model [15].

The parameters in LUARLW are tuned to reproduce 14 distributions of kinematic variables over the entire energy region covered by the scan [14, 16]. For example, the fits for parameters tuned at $E_{\text{cm}} = 2.2$ GeV are shown in Figure 5. We find that one set of parameter values is required for the CM energy region below open charm threshold, and that a second set is required for higher energies. In an alternative approach, the parameter values were tuned point-by-point throughout the entire energy range. The detection efficiencies determined using individually tuned parameters are consistent with those determined with globally tuned parameters to within 2%. This difference is included in the systematic errors. The detection efficiencies were also determined using JETSET74 for the energies above 3 GeV. The difference between the JETSET74 and LUARLW results is about 1%, and is also taken into account in estimating the systematic uncertainty. Figure 6 shows the variation of the detection efficiency as a function of CM energy.

3.4. Radiative Corrections: $(1 + \delta)$

The $(1 + \delta)$ term is necessary to remove high order effects from $\sigma_{\text{had}}^{\text{obs}}$

$$\sigma_{\text{had}}^{\text{obs}} = \sigma_{\text{had}}^o \cdot \varepsilon_{\text{had}} \cdot (1 + \delta)$$

Table I Some values used in the determination of R at a few typical energy points.

E_{cm} (GeV)	N_{had}^{obs}	N_{ll+} $N_{\gamma\gamma}$	L (nb^{-1})	ε_{had} (%)	$(1 + \delta)$	R	Stat. error	Sys. error
2.000	1155.4	19.5	47.3	49.50	1.024	2.18	0.07	0.18
3.000	2055.4	24.3	135.9	67.55	1.038	2.21	0.05	0.11
4.000	768.7	58.0	48.9	80.34	1.055	3.16	0.14	0.15
4.800	1215.3	92.6	84.4	86.79	1.113	3.66	0.14	0.19

Table II Contributions to systematic errors: hadronic selection, luminosity determination, hadronic efficiency determination, trigger efficiency, radiative corrections and total systematic error. All errors are in percentages (%).

E_{cm} (GeV)	Had. sel.	L	Had. eff.	Trig.	Rad. corr.	tot.
2.000	7.07	2.81	2.62	0.5	1.06	8.13
3.000	3.30	2.30	2.66	0.5	1.32	5.02
4.000	2.64	2.43	2.25	0.5	1.82	4.64
4.800	3.58	1.74	3.05	0.5	1.02	5.14

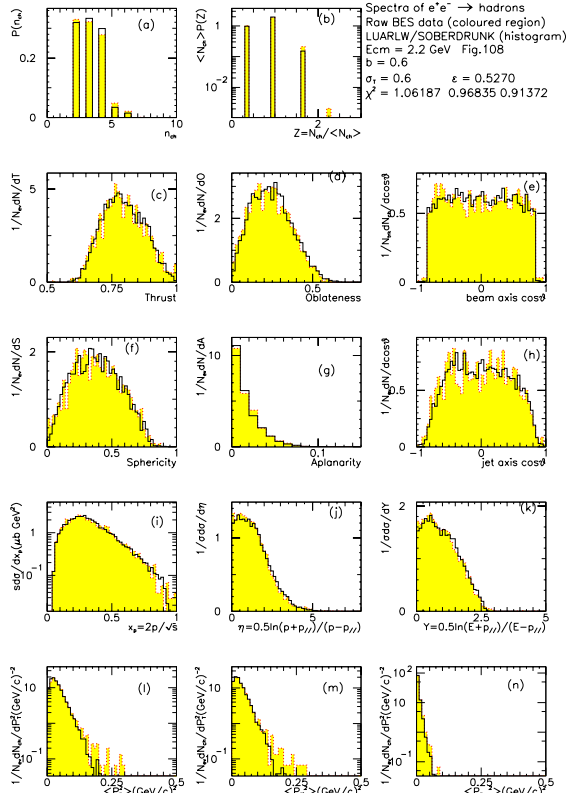


Figure 5: Comparison of BES data (shaded histogram) and LUARLW Monte Carlo data (black histogram) tuned for 2.2 GeV scan point.

Different schemes for the radiative corrections were compared [17–20], as reported in [12]. Below charm threshold, the four different schemes agree with each other to within 1%, while above charm threshold, where resonances are important, the

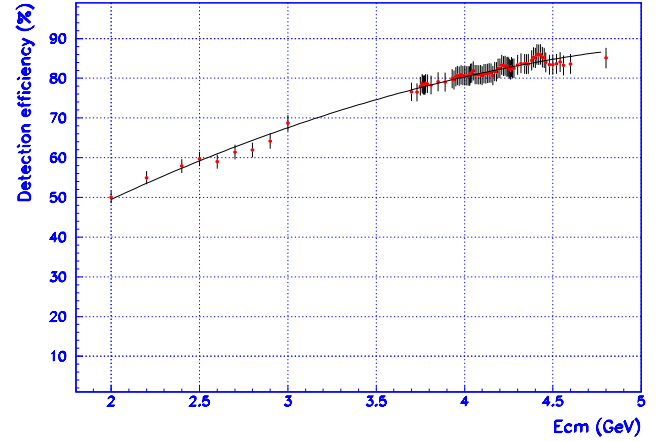


Figure 6: The cm energy dependence of the detection efficiency for hadronic events estimated using the LUARLW generator. The error bars are the total systematic errors.

agreement is within 1 to 3%. The radiative correction used in this analysis is based on [20], and the differences with the other schemes are included in the systematic error.

3.5. Luminosity Measurement

The integrated luminosity is determined from

$$L = \frac{N_{obs}}{\sigma \varepsilon \varepsilon_{trg}}$$

using Bhabha events. The results obtained using $\gamma\gamma$ and dimu events were consistent. The luminosity systematic error includes contributions from cut variations, background uncertainties, the cross section uncertainty, and the efficiency un-

certainty. The luminosity systematic errors at some selected scan energies are shown in Table II.

3.6. Trigger Efficiency

The trigger efficiency was measured by comparing different trigger configurations in special runs at the J/ψ .

$$\begin{aligned}\varepsilon_{\text{Bhabha}} &= 99.96\% \\ \varepsilon_{\mu\mu} &= 99.33\% \\ \varepsilon_{\text{had}} &= 99.76\%\end{aligned}$$

The error on the efficiencies is 0.5%.

3.7. BES Results

The BES R measurement results [12, 21] are shown in Figure 7 along with the results from $\gamma\gamma 2$, Mark I, and Pluto [22–24]. Systematic uncertainties are between 6 and 10% and are less than half of the previous uncertainties. The average uncertainty is 6.6%. Tables I and II list some of the values used in the determination of R and the contributions to the uncertainty in the value of R at a few typical energy points in the scanned energy range, respectively.

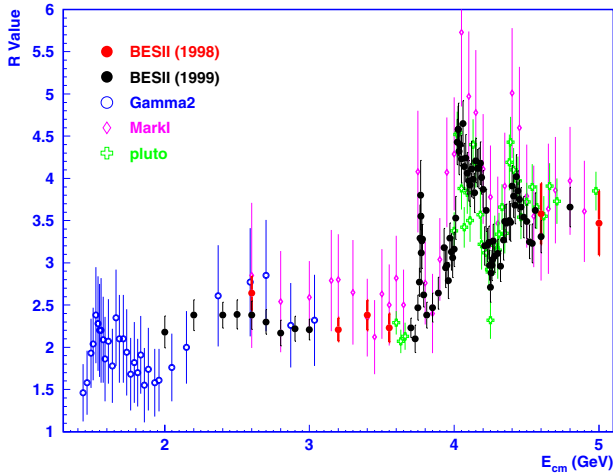


Figure 7: A compilation of measurements of R in the cm energy range from 1.4 to 5 GeV. In addition to the BES results [12, 21], results from $\gamma\gamma 2$, Mark I, and Pluto [22–24] are shown.

4. RECENT CLEO MEASUREMENT

The CLEO experiment measured R at $E_{\text{cm}} = 10.52$ GeV, just below the $\Upsilon(4S)$, and obtained $R = 3.56 \pm 0.01 \pm 0.07$ [25]. This very precise measurement (2%) obtained an error similar to that of all previous results in this energy region combined, $\bar{R} = 3.579 \pm 0.066$, corresponding to a 1.8 % error [26]. Fig. 8 shows the measurements in this region prior to CLEO [26].

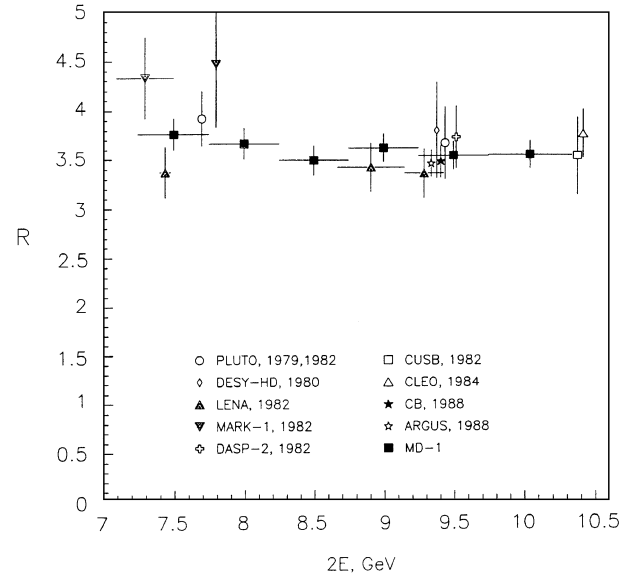


Figure 8: R measurements in the 7 to 10 GeV energy region. Plot from [26].

The CLEO error is smaller than that obtained by BES. A breakdown of the error components is given in Table III, along with the corresponding errors at 3.0 GeV from BES. Why does CLEO do better? CLEO has much better solid angle coverage and a higher detection efficiency, as well as a state of the art detector. They also ran with a higher luminosity, 1.521 ± 0.015 fb $^{-1}$, and obtained 4 million events. With a much bigger sample, both statistical and systematic errors are reduced.

5. CURRENT STATUS OF R MEASUREMENTS

Burkhardt and Pietrzyk have updated their analysis from 1995 [9] with new results from CMD-2, CLEO, BES, and 3rd order QCD for $E_{\text{cm}} > 12$ GeV [6]. They find $\alpha^{-1}(M_Z^2) = 128.936 \pm 0.046$, and $\Delta\alpha_{\text{had}}^{(5)} = 0.02761 \pm 0.00036$. In 1995, $\Delta\alpha_{\text{had}}^{(5)} = 0.0280 \pm 0.0007$. The improved experimental accuracy is primarily due to BES [6]. Figure 9 shows their current summary of R measurements below 10 GeV. The error in the 2 to 5 GeV region is greatly reduced because of the BES measurements. Figure 10 shows the breakdown of the error in $\Delta\alpha(M_Z^2)$ by energy region. The biggest error contribution to $\Delta\alpha_{\text{had}}^{(5)}$ still comes from the $1 < E_{\text{cm}} < 5$ GeV region!

FUTURE R MEASUREMENTS

J.H. Kühn has used the new BES results to test PQCD, but calls for even better precision (2%) [2]. Certainly, the precision of R in the 1–2 GeV cm region must be improved. This is extremely important to improve the precision of both a_μ and $\alpha(M_Z^2)$. The KLOE and PEP-N experiments are candidates for measuring R in this region.

Table III Comparison of R systematic error contributions between BES (at 3.0 GeV) and CLEO (at 10.52 GeV).

Source	BES (%) Error (%)	CLEO Error (%)
N_{had}	3.3	–
Backgd./Ev. Modeling	–	0.7
L	2.3	1.0
$1 + \delta$	1.3	–
ε_{had}	2.7	–
$\varepsilon_{\text{had}} \times (1 + \delta)$	–	1.0
Sys.	5.0	1.8
Stat.	2.5	0.3
Total	5.6	2.0

As shown in Figure 10, the 2–5 GeV region is also very important in the determination of $\Delta\alpha(M_Z^2)$. The candidates for R measurements in this region are BES, PEP-N, and CLEO-C. Also improved measurements in this region are important to clarify the structure in the charm resonance region. The B Factories may also contribute to both energy regions using ISR events [27, 28].

The 5–7 GeV region is also very important. As shown in Figure 9, the R values used by theorists in this region are the unpublished Crystal Ball values [7]. CLEO-C could measure points in this region.

What is needed to improve R value precision?

1. High luminosity \rightarrow large sample
2. Good solid angle coverage
3. Excellent detector with good particle identification
4. Radiative correction to better than 1%
5. More effort on the event generator (LUARLW)
6. Large sample for tuning the generator
7. Measure exclusive channels at low energy

6. ENERGY REACH OF PEP-N

Although very difficult, extending the energy range to above the mass of the $\psi(2S)$ should be considered. Currently the world's largest sample (~ 4 M events) is that of the BES experiment. Some very good physics becomes accessible in this region. $\tau\tau$ production at threshold can be measured to improve the precision of the τ mass. Approximately one quarter of $\psi(2S)$ decays are to χ_c and η_c . Running on the $\psi(2S)$ is a good place to do χ_c and η_c physics, as well as to study $\psi(2S)$ hadronic decays. The study of the hadronic decays might provide a solution to the well known $\rho\pi$ puzzle [29]. Being able

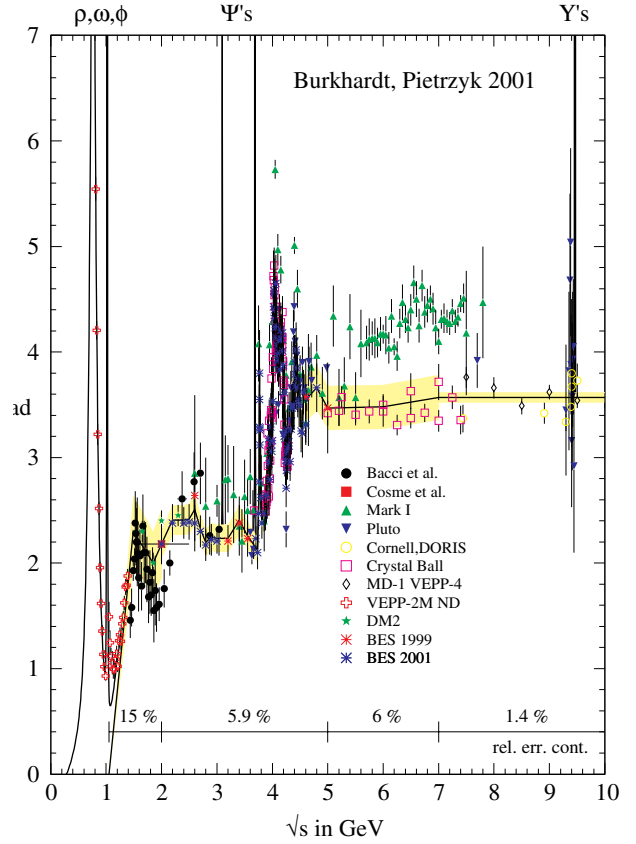


Figure 9: Summary of current R values from [6]. Compare with Figure 2.

to compare J/ψ and $\psi(2S)$ decays is also very beneficial in understanding the final states in these decays. Finally it will be very useful to have some overlap between PEP-N and CLEO-C as a check of systematics in measuring R in this region.

7. SUMMARY

Although the precision of R measurements has improved, better R precision is still needed to improve the precision of the theoretical standard model values of a_μ and $\alpha(m_Z^2)$ and to test PQCD. There are many interesting possibilities for future improvements of R values from KLOE, PEP-N, and CLEO-C, as well from the B factories using ISR events.

8. ACKNOWLEDGEMENTS

I would like to thank the organizers of the e^+e^- Physics at Intermediate Energies Workshop for their hospitality. I also want to thank Bolek Pietrzyk for many of the plots used in this paper and my friend and collaborator Zhengguo Zhao, who is the leader of the R-Group, for his help on this paper. I also want to acknowledge the efforts of the BES R-group, the Computing Group at IHEP, the BEPC staff, and the members of the BES collaboration.

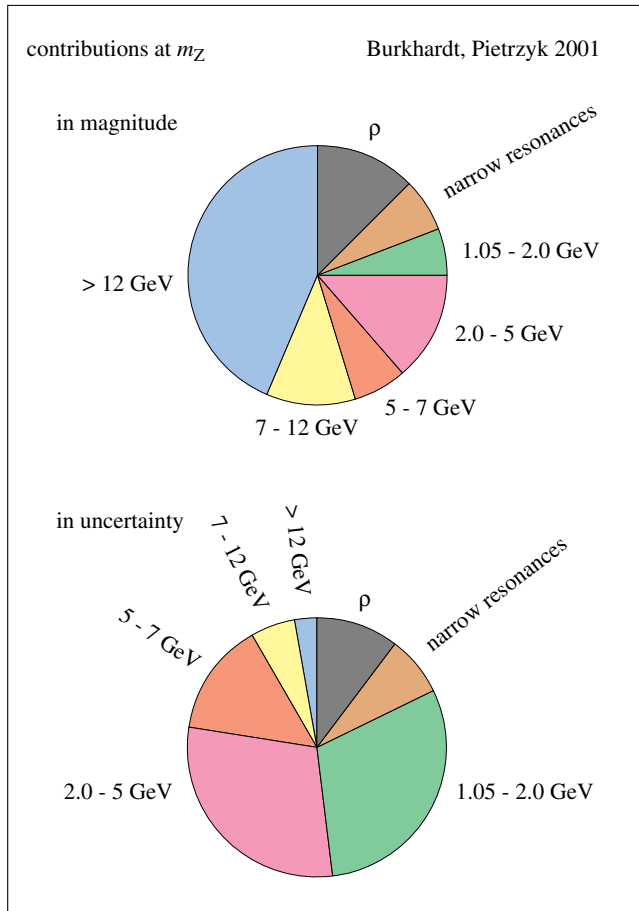


Figure 10: Contributions to $\Delta_{\text{had}}^{(5)}(m_Z^2)$ from the various energy regions in magnitude and in uncertainty. Figure from [6].

REFERENCES

[1] W. Marciano, “General Talk on Hadronic Corrections in the SM,” *The e^+e^- Physics at Intermediate Energies Workshop*, M06.
 [2] J. H. Kühn, “Hadronic Corrections to $\alpha(M_Z^2)$ and g_μ , Theory and Experimental Data,” *The e^+e^- Physics at Intermediate Energies Workshop*, M08.
 [3] S. Eidelman, “Status of CVC Tests from Electron-Positron Annihilation and τ Decay,” *The e^+e^- Physics at Intermediate Energies Workshop*, M07.
 [4] Z. Zhengguo, “Results and Future Plans from BEPC,” *The e^+e^- Physics at Intermediate Energies Workshop*, M10.
 [5] Particle Data Group, D.E. Groom et al., *Eur. Phys. J. C* **15**, 1 (2000).

[6] H. Burkhardt and B. Pietrzyk, accepted by *Phys. Lett. B*, LAPP-EXP 2001-03 (Feb. 2001).
 [7] C. Edwards et al., SLAC PUB 5160 (1990).
 [8] M. Davier and A. Hoecker, *Phys Lett.* **B419**, 419 (1998).
 [9] H. Burkhardt and B. Pietrzyk, *Phys. Lett.* **B356**, 398 (1995).
 [10] Z.G. Zhao, *International Journal of Modern Physics*, **A15**, 3739 (2000).
 [11] J.Z. Bai et al., (BES Collab.), *Nucl. Instr. Methods* **A458**, 627 (2001).
 [12] J. Z. Bai et al., (BES Collab.), *Phys. Rev. Lett.* **84**, 594 (2000).
 [13] B. Andersson and Haiming Hu, “Few-body States in Lund String Fragmentation Model,” hep-ph/9910285.
 [14] For a more complete description of LUARLW see Haiming Hu, “Hadron Production at Intermediate Energies,” *The e^+e^- Physics at Intermediate Energies Workshop*, T24.
 [15] E. Eichten et al., *Phys. Rev.* **D21**, 203 (1980).
 [16] Haiming Hu et al., “The Application of A New Generator Based on Lund Area Law to the R Scan in 2-5 GeV Center-of-mass Energy Region,” Accepted by “High Energy Physics and Nuclear Physics (China).”
 [17] F.A. Berends and R. Kleiss, *Nucl. Phys.* **B178**, 141 (1981).
 [18] G. Bonneau and F. Martin, *Nucl. Phys.* **B27**, 387 (1971).
 [19] E. A. Kuraev and V.S. Fadin, *Sov. J. Nucl. Phys.* **41**, 3 (1985).
 [20] A. Osterheld et al., SLAC-PUB-4160, 1986. (T/E)
 [21] J. Z. Bai et al., (BES Collab.), submitted to PRL, hep-ex/102003.
 [22] C. Bacci et al., ($\gamma\gamma 2$ Collab.), *Phys. Lett.* **B86**, 234 (1979).
 [23] J. L. Siegrist et al., (Mark I Collab.), *Phys. Rev.* **D26**, 969 (1982).
 [24] L. Criegee and G. Knies, (Pluto Collab.), *Phys. Rep.* **83**, 151 (1982);
 Ch. Berger et al., *Phys. Lett.* **B81**, 410 (1979).
 [25] R. Ammar et al., CLEO Collab., *Phys. Rev.* **D57**, 1350 (1998).
 [26] A. E. Blinov et al., *Z. Phys.* **C70**, 31 (1996).
 [27] T. Benninger, X.C. Lou, and W. M. Dunwoodie, “Physics with ISR EVENTS at B Factory Experiments.”
 [28] E. Solodov, Study of the 1.5–3 GeV region using ISR with BaBar,” *The e^+e^- Physics at Intermediate Energies Workshop*, T03.
 [29] M. Suzuki, *Phys. Rev.* **D63**, 054021 (2001).